Scripta Materialia 227 (2023) 115312

Contents lists available at ScienceDirect

Scripta Materialia

journal homepage: www.journals.elsevier.com/scripta-materialia

Nanoindentation avalanches and dislocation structures in HfNbTiZr high entropy alloy

Yu-Zhen Yin [a], Yan Lu [a], Tai-Ping Zhang [b], Wei-Zhong Han [a,*]

[a] Center for Advancing Materials Performance from the Nanoscale, State Key Laboratory for Mechanical Behavior of Materials, Xi'an Jiaotong University, Xi'an 710049, China

[b] School of Materials Science and Engineering, North China University of Water Resources and Electric Power, Zhengzhou 450045, China

ARTICLE INFO

Keywords:
High entropy alloy
Nanoindentation
Avalanche
Dislocation
Mobility

ABSTRACT

High temperature nanoindentation was performed on a refractory HfNbTiZr high-entropy alloy to probe the unique dislocation behaviors. Anomalous nanoindenation avalanche occurs once the load reaches a critical value of 10 mN and exceeds the elastic limit of the alloy. The depth of the plastic zone under indentation is much deeper in the sample with avalanches, and continues to deepen with the increase of testing temperature. A large fraction of mixed dislocations is formed after nanoindentation, instead of forming the long screw dislocations as in common refractory metals. Nanoindentation avalanche is induced by the sudden movement of a group of usually sluggish dislocations, which have a low mobility due to local chemical fluctuations and large lattice distortions. These results manifest a weak temperature-dependence of dislocation mobility in body-centered cubic high-entropy alloy.

The plasticity of metals is usually mediated by dislocation motion [1].According to the interaction angle between dislocation line and the Burgers vector, there are two typical dislocations, namely edge dislocation and screw dislocation. For face-centered cubic metals, the mobility of edge dislocation and screw dislocation is similar. However, for body-centered-cubic (BCC) metals, the a/2<111> screw dislocation glides much slower than the edge dislocation because of their unique three-dimensional core structure, and its motion is highly temperature-dependent and relies on the nucleation and expansion of kink-pairs [2,3]. In general, the glide of screw dislocations needs to overcome a high energy barrier compared with the edge dislocations in BCC metals [4,5].

For BCC high-entropy alloys (HEAs), large lattice distortions and chemical concentration fluctuations induced by multiple alloying elements make the dislocation motion different from that of common BCC metals. A clear understanding of the unique dislocation behavior in BCC HEAs is a prerequisite for understanding and tuning their plasticity. Recently, several efforts have been made to explore the dislocation behavior in BCC HEAs [6–10]. It is found that the concentration fluctuations in HEAs could pin dislocations and promote their cross-slip in BCC HEAs, which is thought to be the key reason for their high ductility [11]. The local composition fluctuations in HEAs play a duplex pinning role in the expansion of both screw and edge dislocations [12]. The dislocation mobility is low under the low load, while both screw and edge dislocations could move quickly when a high load is applied [13]. The small gap of slipping resistance between each low-order slip plane in HEAs is conducive to initiating multiple slip planes and enhancing the deformability [14]. Concentration waves in HEAs contribute to the spontaneous kink-pair nucleation at room temperature, thus the nucleation of kink-pair is no longer a limiting factor for the motion of screw dislocations, while the expansion of kinks and the failure of cross-kinks are the limiting factors [15]. But there is no unified understanding and the critical experimental evidences are lacking.

Nanoindentation is an effective method to study the nucleation, motion and evolution of dislocations in metals [16–20]. The strain burst usually occurs at the end of elastic loading in the nanoindentation of pure metals, which is characterized by nucleation and glide of dislocations. The initial plasticity in FeCoCrMnNi indicates that the nucleation of dislocations is the result of the cooperative motion of multiple atoms [21]. A careful study of the dislocation structures under the indentation of a MoNbTi revealed the initiation of higher-order slip planes and the residual of the edge dislocations [14]. However, due to chemical composition fluctuation and high lattice distortion, strain bursts in the nanoindentation of BCC HEAs are thought impossible.

* Corresponding author.
E-mail address: wzhanxjtu@mail.xjtu.edu.cn (W.-Z. Han).

https://doi.org/10.1016/j.scriptamat.2023.115312
Received 13 December 2022; Received in revised form 12 January 2023; Accepted 17 January 2023
Available online 21 January 2023

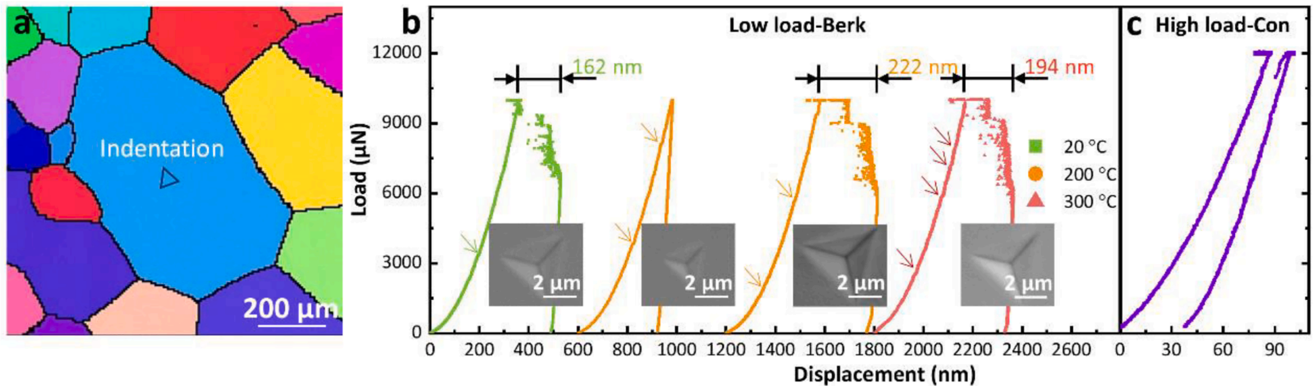

Fig. 1. Nanoindentation of HfNbTiZr alloy. (a) Orientation map of initial grains. Nanoindentations were performed in the middle large grain with normal axis of [245]. (b) Load-displacement curves and indentation morphology of the sample using a low load Berkovich indenter at different testing temperatures. (c) Load-displacement curve of sample under a high load conical indenter at room temperature.

Here, we investigate the plasticity of a refractory HfNbTiZr HEA using high temperature nanoindentation. It is found that an anomalous nanoindentation avalanche occurs once the load reaches a critical value. The avalanche arises from the enhanced dislocation glide ability under high load. Moreover, the relative mobility of screw versus edge dislocations in HEAs increases with temperature, but it is less temperature-dependent than simple BCC metals.

HfNbTiZr is used as a model material to study the dislocation behavior in BCC HEAs. The initial sample has a BCC single-phase structure, as shown by the X-ray diffraction pattern in Fig. S1b. The average grain size is about several hundred micrometers (Fig. S1a), which is large enough to conduct nanoindentation tests in a single grain. In this study, all nanoindentations were performed in a grain with [245] normal orientation (Fig. 1a) in the temperature range of 20 °C to 300 °C using a Hysitron TI950 Triboindenter with an Xsol high temperature heating stage. All nanoindentation tests were conducted in an argon-hydrogen mixture atmosphere to reduce sample from oxidation. A constant loading rate of 2 mN/s was used for Berkovich indenter test, and a slightly higher loading rate of 2.4 mN/s was adopted for conical indenter tests. Nanoindentations are performed at least three times for each temperature. The indentation spacing is set to 50 μm to prevent possible interference between indentations.

In nanoindentation, the first occurrence of displacement burst is called pop-in [22], which indicate that the stress has reached the threshold of dislocation nucleation or the critical gliding stress of pre-existing dislocations [23–25]. In this study, tiny pop-in occurs at load slightly less than 300 μN, indicating the change from elastic deformation to plastic deformation. With the load increasing, there are only some very tiny strain bursts on the load-depth curve, as marked by arrows in Fig. 1b. However, once the load reaches about 10 mN, an extremely large strain burst appears, while the critical load is much larger than the first pop-in load. The burst size is about 162 nm at 20 °C, which is at least one order of magnitude larger than the burst displacement for normal pop-in [17]. According to the load-displacement curve, once the maximum load achieves 10 mN, the avalanche occurs immediately and continues during the load holding process. This observation manifests that 10 mN is the critical load for the avalanche. We also plot one curve without avalanche at 200 °C to show the unique behavior of the special strain burst phenomenon. Here, we refer this phenomenon as *nanoindentation avalanches*. In our tests, 21 out of 25 nanoindentations show such avalanches during the initial loading, which mean it is a general behavior in HfNbTiZr. The nanoindentation avalanches was found in tests ranging from 20 to 300 °C. The shape of indentations after avalanches are clear and look like as the normal ones, as shown in Fig. 1b. The unique nanoindentation avalanches are also confirmed in HfNbTiZr when using a high-load conical indenter,

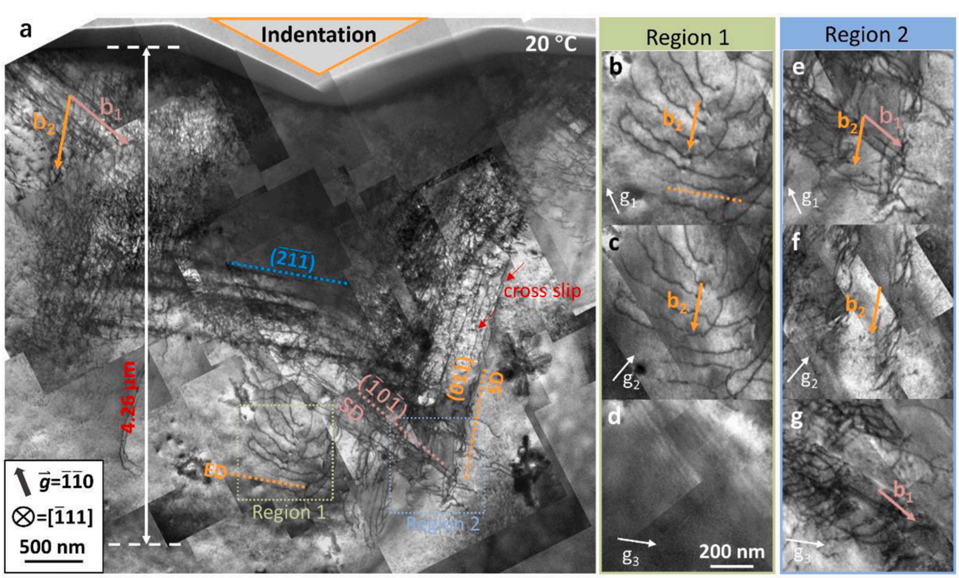

Fig. 2. (a) Dislocation structures underneath the indentation with avalanche formed at 20 °C. (b-d) Dislocation structures in region 1 under three different diffraction **g** vector. (e-g) Dislocation structures in region 2 under three different diffraction **g** vector.

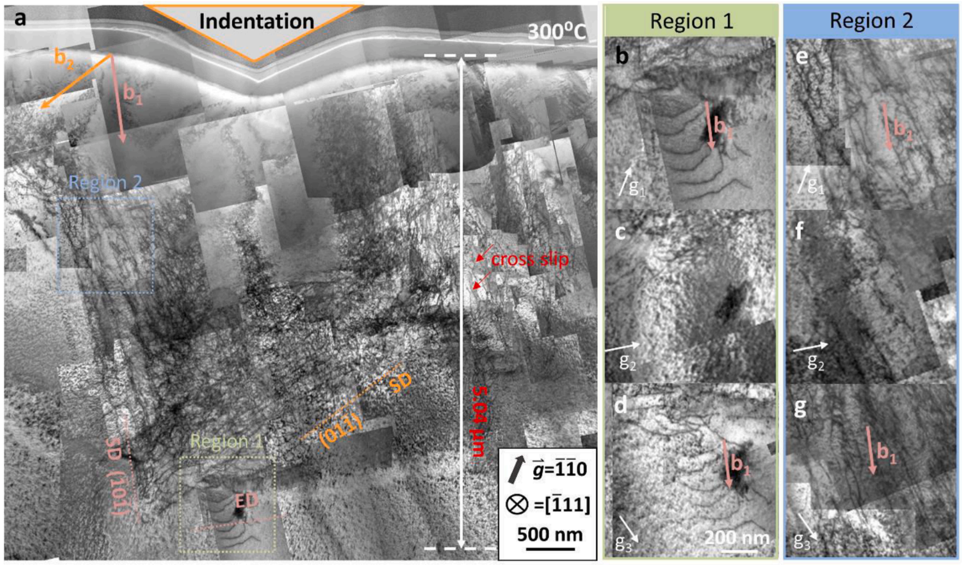

Fig. 3. (a) Dislocation structures underneath indentation with avalanche formed at 300 °C. (b-d) Dislocation structures in region 1 under three different diffraction **g** vector. (e-g) Dislocation structures in region 2 under three different diffraction **g** vector.

although the critical load for the avalanches is slightly larger (due to a larger tip radius of the conical indenter), as shown in Fig. 1c. This indicates that nanoindentation avalanche is an intrinsic property of the HfNbTiZr HEA.

To investigate the origin of such avalanches and their correlation with the dislocation behavior in HfNbTiZr, we carefully studied the dislocation structures underneath three typical indentations: the indentations with the avalanche at 20 °C and at 300 °C, and the indentation without avalanche at 200 °C. We use focused ion beam (FIB) to cut a thin foil sample at the position just below the indentations and characterize dislocation structures using a JEOL 2100 transmission electron microscope (TEM). To minimize Ga^+ damage caused by the FIB, flashing electrolytic polishing of the lift-out sample was performed in a methanol solution of 10 vol% perchloric acid at a voltage of 10 V and at −40 °C for 300 ms.

Fig. 2 shows the dislocation structures underneath the indentation

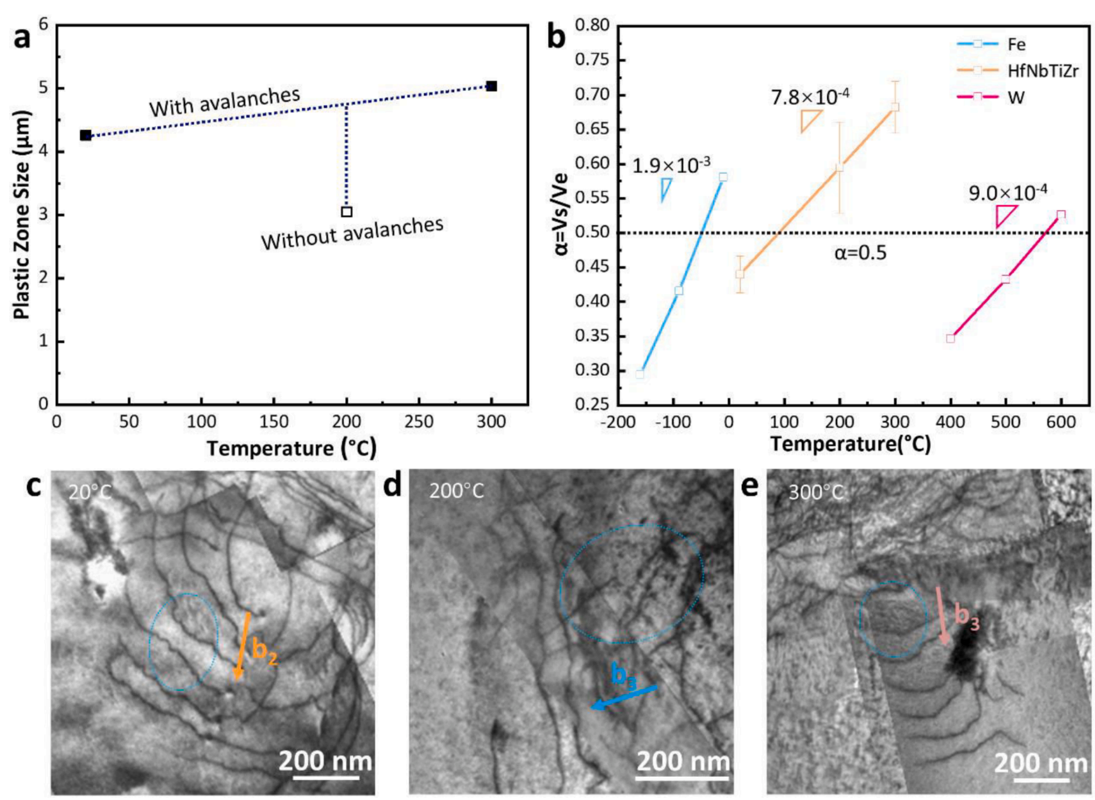

Fig. 4. (a) Depth of plastic zone for three samples: with avalanches at 20 °C, without avalanches at 200 °C, and with avalanches at 300 °C. (b) Variation of the relative mobility of screw versus edge dislocations with temperature for HfNbTiZr, Fe and W. (c-e) Determining the relative mobility of screw versus edge dislocations based on the bowing-out shape of dislocations in HfNbTiZr.

with avalanche formed at 20 °C. Holistic analyses of the dislocation Burgers vector and dislocation types were performed in the plastic zone underneath the indentation, as shown in Figs. 2a, S2 and S3. Some typical dislocations are marked in Fig. 2a, and dislocations with Burgers vector of $b_1=1/2[\bar{1}0\bar{1}]$ are indicated by pink arrows, while dislocations with $b_2=1/2[01\bar{1}]$ are colored in orange arrow. The depth of the plastic zone under the indentation is about 4.26 µm. Except for dislocations, there are no signs of deformation twins and phase transformation under the indentation. Therefore, the nanoindentation avalanche at 20 °C is mediated by dislocations. Two types of slip planes are identified at room temperature according to the dislocation traces, including {110} and {112} planes. Dislocation glide occurs on three (110) planes but only on one (112) plane. The co-activation of dislocations on {112} and {110} planes indicates that the Peierls stress is close for the two slip planes [26].

As shown in Fig. 2, most of the slip bands display an edge-on state, specifically in the form of narrow and straight dislocation. The region 1 highlights dislocations on a face-on (110) slip band. The dislocation structures in region 1 are viewed under three different diffraction vectors (**g**), as shown in Fig. 2b to d. The dislocations have a wavy shape and most of them have a mixed character, and no long pure edge or screw dislocations are observed. Due to the large lattice distortion or chemical short range order in HEAs, the movement of dislocations is sluggish, and drags out many tiny dislocation jogs along the line [27, 28]. Region 2 shows the dislocation structures at the end of the plastic zone. Only the dislocations on {110} are activated, and these dislocations have the characteristics of both the pure screw and mixed type. Some screw dislocations show significant cross-slip behavior, as indicated in Fig. 2a. Dislocation cross-slip is an efficient way to induce multiple-slip, which further enhances the plasticity of alloy.

To explore the dislocation structure of nanoindentation avalanche at higher temperature, a thin foil underneath indentation with avalanche at 300 °C was lifted out and characterized, as shown in Fig. 3. The Burgers vector of dislocations are determined using the different two beam conditions in Figs. S6-S8. The depth of the plastic zone is about 5.04 µm. Denser {110} dislocation slips are initiated at 300 °C, and the dislocation entanglement is more pronounced. Moreover, the cross-slip occurs more frequently, as shown in Fig. 3a. Dislocation glide on {112} plane is also observed. The analysis of the dislocations in region 1 and 2 shows that the Burger vectors of the dislocations are 1/2{110}< 111> and most of them have a mixed character.

Compared to the sample with avalanche, the deformation structure under the indentation of HfNbTiZr without avalanche is shown in Fig. S4. The whole deformation zone is similar to the one in Fig. 2, but there are some differences. First, the depth of the plastic zone is shallow, only 3.05 µm, which indicates that the avalanche corresponds to a large number of dislocations gliding to deeper regions. Second, the dislocation structure at the bottom of the indentation after avalanche shows a triangular shape (Figs. 2 and 3), which is different from the square shape plastic zone for the test without avalanche.

Fig. 4a plots the relationship between the size of plastic zones with and without avalanches and temperature. The plastic zone size of the sample without avalanche at 200 °C is only 3.05 µm, which is much smaller than the other two samples with avalanches. This observation well explains the nanoindentation avalanches phenomenon. In general, the velocity of dislocation in metals is stress-dependent [13]. The dislocation mobility is slow under low load, while both the screw and edge dislocations could move quickly, and their velocities increase linearly with the applied stress [13]. Before avalanche occurring, dislocations have a low mobility due to high Peierls stress induced by local chemical fluctuations and large lattice distortions. Once the load reaches a certain threshold of about 10 mN, the high stress drives plenty of dislocations glide suddenly and rapidly, resulting in a large variation in the indentation depth, which causes the avalanche, as shown in Fig. 1. This is also the reason why the dislocation structure at the bottom of the plastic zone after avalanche displays a triangular shape-interacting of two main glide planes. During avalanche, frequent dislocation cross-slip is also activated to coordinate plastic strains (Figs. 2 and 3).

Some BCC metals exhibit brittleness even at room temperature, such as Cr, Mo and W, however, the BCC HfNbTiZr HEA shows relatively good plasticity [29–32]. To explain this, we estimate the relative mobility of screw versus edge dislocations and plot it in Fig. 4b. Ductile deformation requires the nucleation and movement of massive dislocations [18]. The latter then demands effective dislocation sources and easy cross-slips, which in turn relies on a sufficiently high screw-to-edge dislocation velocity ratio to operate efficiently. The screw-to-edge dislocation velocity ratio can be estimated based on the geometrical shape of dislocations [18]. According to the dislocation shape on the face-on (110) slip plane in Figs. 4c-e, the relative mobility of screw versus edge dislocation α can be determined, as shown in Fig. 4b. For BCC metals, the material exhibits toughness once the α is larger than 0.5 [18]. HfNbTiZr has an α value of 0.43 at room temperature, which is due to the lower relative mobility of screw versus edge dislocations compared with most simple BCC metals [33]. The value is very close to the critical value of 0.5, thus showing reasonable ductility [12]. In addition, frequent cross-slips induced multiple-slip might be another reason for the high deformability of HfNbTiZr (Figs. 2 and 3). The concentration fluctuation in HEAs can pin dislocations and promote their cross-slip, which is considered as the key reason for the high ductility of BCC HEAs [11]. The dislocations produced under the indentation have a mixed character, containing both the screw and edge components (Figs. 2 and 3), which is completely different from the long screw dislocation structures in pure BCC metals [18]. Since edge dislocations move quickly and are easily to be annihilated at the grain boundaries or free surfaces, while screw dislocations move slowly and remain as straight lines [32,34], thus it is difficult to see a large number of mixed dislocations after deformation [35]. This indicates that the difference of mobility between screw and edge dislocations in HfNbTiZr is not obvious compared with that in pure BCC metals [36]. In addition, the slope of the α-temperature curve of HfNbTiZr in Fig. 4b is smaller than that of Fe and W, indicating that the dislocation mobility in HfNbTiZr is less temperature-dependent.

In summary, an unusual avalanche phenomenon occurs during nanoindentation of HfNbTiZr HEA once the critical load reaches 10 mN, which originates from the quick and sudden motion of the usually sluggish dislocations under the high load. The HfNbTiZr HEA exhibits excellent deformation ability because of the relatively high screw-to-edge dislocation velocity ratio and high cross-slip propensity that enables multiple-slip behaviors.

Declaration of Competing Interest

The authors declare that there is no competing financial interest.

Acknowledgement

Y. Z. Yin appreciates the assistance of X. H. Lin, Y. B. Qin, P. C. Zhang and D. L. Zhang in this study. This research was supported by the National Natural Science Foundation of China (Grants 51922082 and 51971170), and the 111 Project of China 2.0 (Grant Number BP0618008).

Supplementary materials

Supplementary material associated with this article can be found, in the online version, at doi:10.1016/j.scriptamat.2023.115312.

References

[1] P.M. Anderson, J.P. Hirth, J. Lothe, Theory of Dislocations, 3rd ed, Cambridge University Press, 2017.
[2] V. Vitek, Core structure of screw dislocations in body-centred cubic metals: relation to symmetry and interatomic bonding, Philos. Mag. 84 (2004) 415–428.

[3] D. Caillard, J.L. Martin, Thermally Activated Mechanisms in Crystal Plasticity, 1st ed., Pergamon, 2003.
[4] J. Chaussidon, M. Fivel, D. Rodney, The glide of screw dislocations in bcc Fe: atomistic static and dynamic simulations, Acta Mater. 54 (2006) 3407–3416.
[5] L. Dezerald, L. Proville, L. Ventelon, F. Willaime, D. Rodney, First-principles prediction of kink-pair activation enthalpy on screw dislocations in bcc transition metals: V, Nb, Ta, Mo, W, and Fe, Phys. Rev. B Condens. Matter Mater. Phys. 91 (2015), 094105.
[6] F. Maresca, W.A. Curtin, Mechanistic origin of high strength in refractory BCC high entropy alloys up to 1900K, Acta Mater. 182 (2020) 144–162.
[7] G. Dirras, J. Gubicza, A. Heczel, L. Lilensten, J.P. Couzinie, L. Perriere, I. Guillot, A. Hocini, Microstructural investigation of plastically deformed $Ti_{20}Zr_{20}Hf_{20}Nb_{20}Ta_{20}$ high entropy alloy by x-ray diffraction and transmission electron microscopy, Mater. Charact. 108 (2015) 1–7.
[8] J.P. Couzinie, L. Lilensten, Y. Champion, G. Dirras, L. Perriere, I. Guillot, On the room temperature deformation mechanisms of a TiZrHfNbTa refractory high-entropy alloy, Mater. Sci. Eng. A 645 (2015) 255–263.
[9] R.R. Eleti, A.H. Chokshi, A. Shibata, N. Tsuji, Unique high-temperature deformation dominated by grain boundary sliding in heterogeneous necklace structure formed by dynamic recrystallization in HfNbTaTiZr BCC refractory high entropy alloy, Acta Mater. 183 (2020) 64–77.
[10] Z.F. Lei, X.J. Liu, Y. Wu, H. Wang, S.H. Jiang, S.D. Wang, X.D. Hui, Y.D. Wu, B. Gault, P. Kontis, D. Raabe, L. Gu, Q.H. Zhang, H.W. Chen, H.T. Wang, J.B. Liu, K. An, Q.S. Zeng, T.G. Nieh, Z.P. Lv, Enhanced strength and ductility in a high entropy alloy via ordered oxygen complexes, Nature 563 (2018) 546–550.
[11] Y.Q. Bu, Y. Wu, Z.F. Lei, X.Y. Yuan, H.H. Wu, X.B. Feng, J.B. Liu, J. Ding, Y. Lu, H. T. Wang, Z.P. Lv, W. Yang, Local chemical fluctuation mediated ductility in body-centered-cubic high-entropy alloys, Mater. Today 46 (2021) 28–34.
[12] B. Chen, S.Z. Li, J. Ding, X.D. Ding, J. Sun, E. Ma, Correlating dislocation mobility with local lattice distortion in refractory multi-principal element alloys, Scr. Mater. 222 (2023), 115048.
[13] B. Chen, S.Z. Li, H.X. Zong, X.D. Ding, J. Sun, E. Ma, Unusual activated processes controlling dislocation motion in body-centered-cubic high-entropy alloys, Proc. Natl. Acad. Sci. USA 117 (2020) 16199–16206.
[14] F.L. Wang, G.H. Balbus, S.Z. Xu, Y.Q. Su, J. Shin, P.F. Rottmann, K.E. Knipling, J. C. Stinville, L.H. Mills, O.N. Senkov, I.J. Beyerlein, T.M. Pollock, D.S. Gianola, Multiplicity of dislocation pathways in a refractory multiprincipal element alloy, Science 307 (2020) 95–101.
[15] F. Maresca, W.A. Curtin, Theory of screw dislocation strengthening in random BCC alloys from dilute to "High-Entropy" alloys, Acta Mater. 182 (2020) 144–162.
[16] J. Varillas, J. Ocenasek, J. Torner, J. Alcala, Understanding imprint formation, plastic instabilities and hardness evolutions in FCC, BCC and HCP metal surfaces, Acta Mater. 217 (2021), 117122.
[17] S.P. Wang, J. Xu, Incipient plasticity and activation volume of dislocation nucleation for TiZrNbTaMo high-entropy alloys characterized by nanoindentation, J. Mater. Sci. Technol. 35 (2019) 812–816.
[18] Y. Lu, Y.H. Zhang, E. Ma, W.Z. Han, Relative mobility of screw versus edge dislocations controls the ductile-to-brittle transition in metals, Proc. Natl. Acad. Sci. USA 118 (2021), e2110596118.
[19] Y.X. Ye, B. Ouyang, C.Z. Liu, G.J. Duscher, T.G. Nieh, Effect of interstitial oxygen and nitrogen on incipient plasticity of NbTiZrHf high-entropy alloys, Acta Mater. 199 (2020) 413–424.
[20] T.D. Wu, Y.H. Cai, T. Wang, J.J. Si, J. Zhu, Y.D. Wang, X.D. Hui, A refractory $Hf_{25}Nb_{25}Ti_{25}Zr_{25}$ high-entropy alloy with excellent structural stability and tensile properties, Mater. Lett. 130 (2014) 277–280.
[21] C. Zhu, Z.P. Lu, T. Nieh, Incipient plasticity and dislocation nucleation of FeCrCoNiMn high-entropy alloy, Acta Mater. 61 (8) (2013) 2993–3001.
[22] A. Gouldstone, N. Chollacoop, M. Dao, J. Li, A.M. Minor, Y. Shen, Indentation across size scales and disciplines: recent developments in experimentation and modeling, Acta Mater. 55 (2007) 4015–4039.
[23] Y. Shibutani, T. Tsuru, A. Koyama, Nanoplastic deformation of nanoindentation: crystallographic dependence of displacement bursts, Acta Mater. 55 (2007) 1813–1822.
[24] A.S. Christopher, Nanoindentation studies of materials, Mater. Today 9 (2006) 32–40.
[25] Y.K. Zhao, J.M. Park, J.I. Jang, U. Ramamurty, Bimodality of incipient plastic strength in face-centered cubic high-entropy alloys, Acta Mater. 202 (2021) 124–134.
[26] S.Z. Xu, Y.Q. Su, W.R. Jian, I.J. Beyerlein, Local slip resistances in equal-molar MoNbTi multi-principal element alloy, Acta Mater. 202 (2021) 68–79.
[27] C. Lee, G. Kim, Y. Chou, B.L. Musico, M.C. Gao, K. An, G. Song, Y.C. Chou, V. Keppens, W. Chen, P.K. Liaw, Temperature dependence of elastic and plastic deformation behavior of a refractory high-entropy alloy, Sci. Adv. 6 (2020) eeaz4748.
[28] R.R. Eleti, N. Stepanov, N. Yurchenko, D. Klimenko, S. Zherebtsov, Plastic deformation of solid-solution strengthened Hf-Nb-Ta-Ti-Zr body-centered cubic medium/high-entropy alloys, Scr. Mater. 200 (2021), 113927.
[29] J.W. Christian, Some surprising features of the plastic deformation of body-centered cubic metals and alloys, Metall. Trans., A, Phys. Metall. Mater. Sci. 14 (1983) 1237–1256.
[30] P. Gumbsch, J. Riedle, A. Hartmaier, H.F. Fischmeister, Controlling factors for the brittle-to-ductile transition in tungsten single crystals, Science 282 (1998) 1293–1295.
[31] J.R. Rice, R. Thomson, Ductile versus brittle behaviour of crystals, Philos. Mag. 29 (1974) 73–97.
[32] Y.H. Zhang, W.Z. Han, Mechanism of brittle-to-ductile transition in tungsten under small-punch testing, Acta Mater. 220 (2021), 117332.
[33] S.I. Rao, B. Akdim, E. Antillon, C. Woodward, T.A. Parthasarathy, O.N. Senkov, Modeling solution hardening in BCC refractory complex concentrated alloys: NbTiZr, $Nb_{1.5}TiZr_{0.5}$ and $Nb_{0.5}TiZr_{1.5}$, Acta Mater. 168 (2019) 222–236.
[34] J. Zhang, W.Z. Han, Oxygen solutes induced anomalous hardening, toughening and embrittlement in body-centered cubic vanadium, Acta Mater. 196 (2020) 122–132.
[35] D. Caillard, Kinetics of dislocations in pure Fe. Part I. In situ straining experiments at room temperature, Acta Mater. 58 (2010) 3493–3503.
[36] S.I. Rao, C. Varvenne, C. Woodward, T.A. Parthasarathy, D. Miracle, O.N. Senkov, W.A. Curtin, Atomistic simulations of dislocations in a model BCC multicomponent concentrated solid solution alloy, Acta Mater. 125 (2017) 311–320.